The Disintegration of Oxygen and Nitrogen by 14.1-Mev Neutrons*

ALAN B. LILLIE
Rice Institute, Houston, Texas
(Received May 26, 1952)

Oxygen and nitrogen contained as a gas in a cloud chamber were bombarded by 14.1-Mev neutrons. From the disintegrations of these nuclei the following data have been collected: (*a*) the range-energy relations of C^{13} in the energy range 0–5 Mev, and the range-energy curve of B^{11} from 0–7 Mev; (*b*) the excited states of the nuclei C^{13}, B^{11}, N^{15}, and N^{16}; (*c*) the angular distributions of the alpha-particles emitted in the $O^{16}(n,\alpha)C^{13}$ and $N^{14}(n,\alpha)B^{11}$ reactions; (*d*) the cross sections for some of the reactions taking place.

I. INTRODUCTION

CLOUD-CHAMBER studies of disintegrations produced by neutrons have been made by several groups. Feather[1] in 1932 studied the $N^{14}(n,\alpha)B^{11}$ reaction; Bonner and Brubaker[2] in 1936 studied the same reaction and the $N^{14}(n,p)C^{14}$ and $N^{14}(n,2\alpha)Li^7$ reactions. These early investigations were limited by the lack of monoenergetic neutron sources. With the availability of tritium, the high energy 14.1-Mev neutrons from the $H^3(d,n)He^4$ reaction opened a new region of study to this older technique. The large cross section for this reaction, obtained with low deuteron energy, makes this a very strong source of monoenergetic neutrons. In addition, since the neutrons are fast and uncharged, their penetrability is high even for large values of angular momentum. For this reason a nuclear level possessing a large spin might be excited by these neutrons, while it might not be found in reactions using slower charged particles of low angular momentum. This present study makes use of these fast neutrons to study the disintegration of oxygen and nitrogen.

II. APPARATUS

The target was tritium absorbed in a zirconium film deposited on a tungsten disk $\frac{1}{2}$ in. in diameter by $\frac{1}{16}$ in. thick.[3] The deuterons were accelerated in the Rice Institute 200-kev Cockroft-Walton accelerator. The neutrons from the $H^3(d,n)He^4$ reaction entered the cloud chamber at 90° to the deuteron beam.

The cloud chamber was 15 cm in diameter by 8 cm deep and of light construction to minimize the scattering of neutrons. The center of the chamber was placed $28\frac{1}{2}$ cm from the center of the target and 95 cm from the floor, which was the nearest large scattering mass.

Tank oxygen and nitrogen having less than one percent impurities filled the cloud chamber to a pressure of one atmosphere. While the recoil protons from the hydrogen present are readily recognizable, disintegrations due to other impurities may not be distinguished from those due to oxygen or nitrogen. Water vapor was therefore used as the vapor in the cloud chamber so that the only nuclei present to more than one percent would be O^{16}, N^{14}, and H^1.

Stereoscopic pictures of the tracks in the cloud chamber were taken and after the film was processed, the images were reprojected through the same optical system. Measurements of track lengths and the angles that the tracks made with the neutrons' paths were made. In addition, the relative track densities in a fork (to aid in the identification of reactions) and the positions in the chamber were noted. All forks were measured provided that the plane of the fork was less than 50° to the horizontal. All recoil nuclei lying within a cone of 10° half-angle for oxygen and 15° half-angle for nitrogen were measured.

Measurements were made to see whether the plane of the fork passed through the target position. This plane would not normally pass through the target position if the disintegration were caused by a scattered neutron. The percentage of forks caused by scattered neutrons was found to be less than four percent.

III. RESULTS

A total of 1600 pictures were taken of disintegrations in oxygen and 2700 pictures of nitrogen. The number of forks (two-particle disintegrations) measured were 1200 in oxygen and 1800 in nitrogen. In the case of nitrogen, 256 tridents (three-particle disintegrations) were also measured. This latter is the disintegration of the nitrogen into two alpha-particles and a Li^7 particle. Figures 1 and 2 show stereoscopic views of disintegrations in oxygen and nitrogen, respectively. In Fig. 1 are several examples of alpha-emission. In Fig. 2 are two cases of three-particle disintegrations, as well as a disintegration in which either a proton or deuteron or triton is emitted, crosses, and leaves the chamber. Some recoil nitrogen nuclei can be seen as very short heavy tracks. An example of alpha-emission is also seen here.

1. Range-Energy Relations

Sufficient numbers of forks for a study of range-energy relations were available from the reactions $O^{16}(n,\alpha)C^{13}$ and $N^{14}(n,\alpha)B^{11}$. The measured length of the heavy particle track in a fork was converted into the range in standard air by multiplying by the stopping power of the gas mixture calculated from the stopping

* This work was supported by the AEC program.
[1] N. Feather, Proc. Roy. Soc. (London) **A136**, 709 (1932).
[2] T. W. Bonner and W. M. Brubaker, Phys. Rev. **49**, 223 (1936).
[3] A. B. Lillie and J. P. Conner, Rev. Sci. Instr. **22**, 210 (1951).

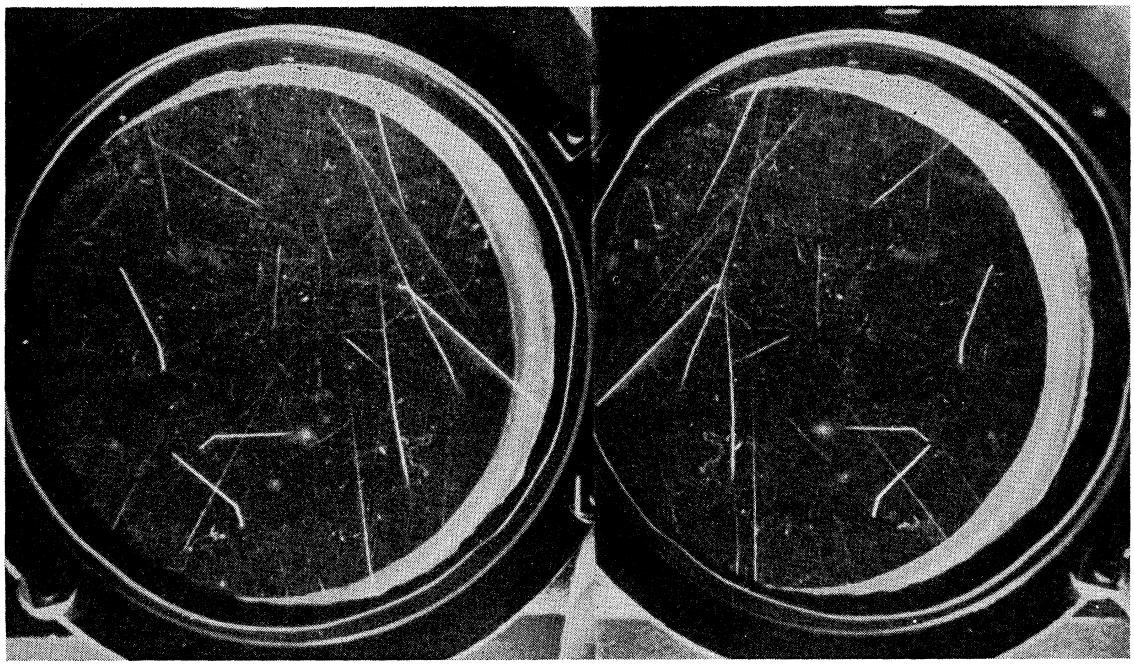

FIG. 1. Stereoscopic picture of disintegrations in oxygen. The neutrons enter from the top of the picture. Several examples of disintegration with alpha-emission can be noted.

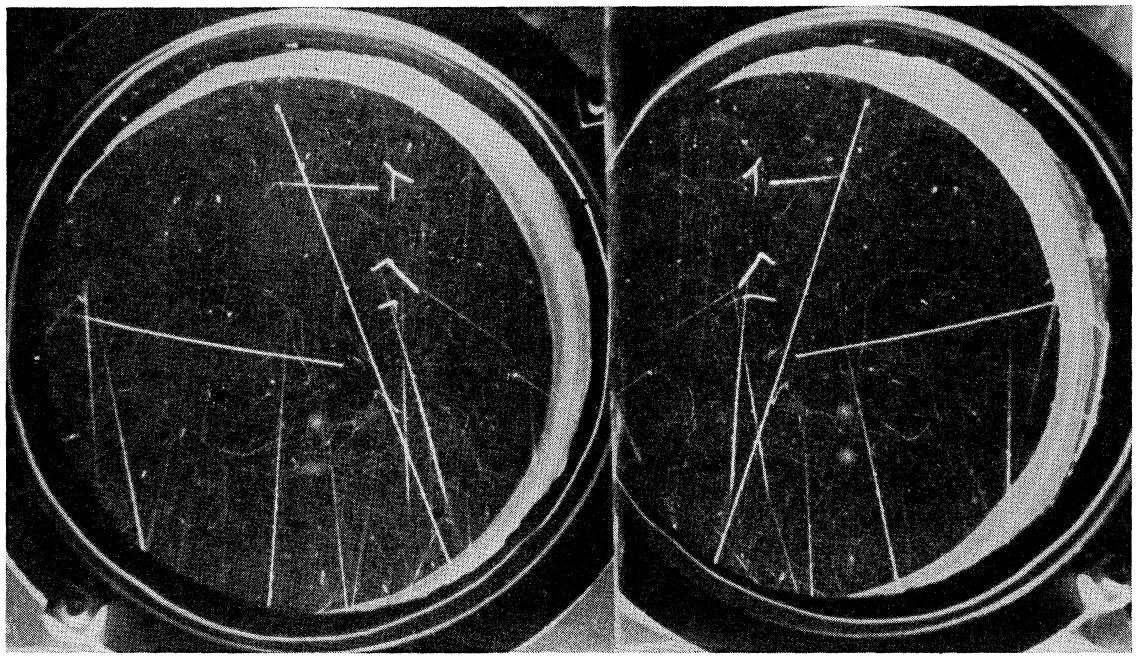

FIG. 2. Stereoscopic picture of disintegrations in nitrogen. The neutrons enter from the top of the picture. Two cases of three-particle disintegration can be seen, as well as a disintegration in which either a proton or deuteron or triton is emitted which crosses and leaves the chamber. Some recoil nitrogen nuclei identifiable as short heavy tracks and an example of alpha-emission are also seen.

powers given by Mano[4] for oxygen, nitrogen, and water. When the excitation energy distributions were plotted later, it was found that the groups were slightly too high in position. The stopping powers were increased by less than two percent to bring the ground level groups into their correct positions of zero excitation energy.

[4] G. Mano, J. phys. et radium **5**, 628 (1934).

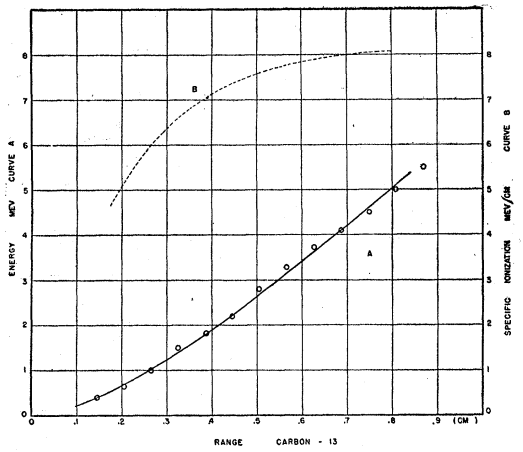

FIG. 3. Curve A: the range-energy curve for a C^{13} particle in air. Curve B: the specific ionization of a C^{13} particle in air as a function of the residual range. This curve is the slope of curve A.

The energy of the heavy particle is calculated by consideration of the momenta involved in the reaction, using the equation

$$M_R E_R = M_n E_n + M_\alpha E_\alpha - 2(M_n M_\alpha E_n E_\alpha)^{\frac{1}{2}} \cos\theta, \quad (1)$$

where M_R, M_n, M_α are the masses of the recoil particle, neutron, and alpha-particle, respectively; E_R, E_n, E_α are the energies of the recoil particle, neutron, and alpha-particle, respectively; and θ is the angle between the alpha-particle track and the neutron's path.

The energy of the alpha-particle is found from the range-energy curves of Bethe.[5] The angle θ is also measured, while the energy of the neutrons and all the mass values are known. The energy of the heavy particle can then be calculated.

The range straggling of the heavy particles, errors in the energies of the alphas, or errors in the angles θ of the alpha tracks contributed to give a considerable spread in range for a given particle energy. To determine the points on the range-energy curve the most probable value of energy for all track lengths in 0.05 cm intervals was plotted *versus* track length. The numbers of tracks in each such interval varied from about 20 to 85 for C^{13}, and from 20 to 100 for B^{11}, there being fewer tracks at high energy. A total of 300 forks for C^{13} and 800 forks for B^{11} were used in these determinations.

Curves A in Figs. 3 and 4 give these range-energy curves for C^{13} and B^{11}, respectively. Curves B in each figure show the specific ionization of the heavy particle as a function of the residual range.

A simple theory[6] indicates that an orbital electron will be lost or captured when the heavy particle has a velocity greater than or less than the effective velocity of that electron. The effective velocity v_{eff} of the most tightly bound electron can be calculated from its ionization potential I by the relation

$$v_{\text{eff}}^2 = 2I/m, \quad (2)$$

where m is the mass of the electron.[7] For carbon and boron these velocities are 13.1×10^8 cm/sec and 10.9×10^8 cm/sec, respectively. The energies of the C^{13} and B^{11} particles with these velocities are 11.7 Mev and 6.9 Mev, respectively. At these energies, when the most tightly bound electron is just lost, the specific ionization is expected to reach a maximum. The ranges for these maximum specific ionizations should be found at about 1.6 cm for C^{13} and at 1.1 cm for B^{11}. The experimental curves for the specific ionizations do not extend over these peaks although that for B^{11} appears to have reached a maximum. Higher particle energies would be necessary to locate the peaks accurately.

To synthesize the range-energy curve for a particle of charge Z and mass M in terms of the range-energy curve for a particle of charge Z_0 and mass M_0, both particles having the same velocity, the approximate relation is[6]

$$R_M(E) = \frac{M}{M_0}\left(\frac{Z_0}{Z}\right)^n R_{M0}\left(\frac{M_0}{M}E\right), \quad (3)$$

where E is the energy of the particle of mass M and n is a parameter dependent on the particles and energies concerned. For velocities of the particles large enough so that all orbital electrons are stripped off (e.g., protons or alphas in the Mev range), this equation is approximately true with $n=2$. The value of n for any two particles may be found by comparing their range-energy curves. The value of n for C^{13} particles and alpha-particles varies from 0.8 for a 0.5-Mev C^{13} particle to 1.0 for a 5-Mev C^{13} particle. For B^{11} particles and alpha-particles the value varies from 1.0 for a 0.5-Mev B^{11} particle to 1.2 for a 7-Mev B^{11} particle.

For C^{13} and B^{11} particles the value of n varies from 0.5 to 0.6 for the C^{13} energy range 0.5 Mev to 5 Mev.

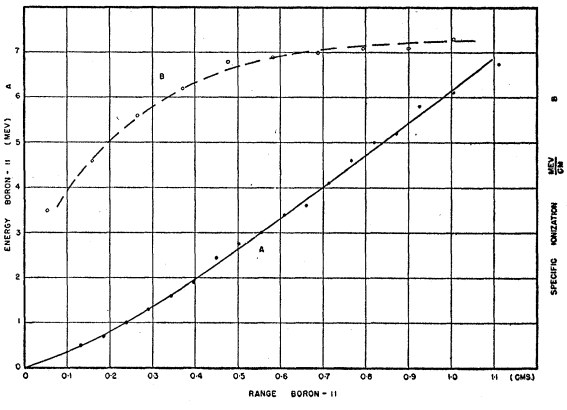

FIG. 4. Curve A: the range-energy curve for a B^{11} particle in air. Curve B: the specific ionization of a B^{11} particle in air as a function of the residual range. This curve is the slope of curve A.

[5] H. A. Bethe, Revs. Modern Phys. **22**, 213 (1950).

[6] N. Bohr, Kgl. Danske Videnskab. Selskab, Mat.-fys. Medd. **18**, No. 8 (1948).

[7] C. E. Moore, *Atomic Energy Levels*, National Bureau of Standards Circular No. 467 (1949), Vol. I.

Blackett,[8] studying O^{16} and N^{14} recoils, found a value of $\frac{1}{2}$ for n between these particles in a similar energy range. In the case where the recoils are much heavier than the atoms of the stopping gas, Bohr gives a theoretical value of $\frac{2}{3}$ for the charge dependence of the range of particles with the same velocity.

2. Calculation of the Energy of Excited States

When a disintegration is produced by a neutron, often the residual heavy nucleus is left excited. The excitation energy can be calculated by the relation

$$E_x=Q_0+E_n(1-M_n/M_R)-E_\alpha(1+M_\alpha/M_R) +2(M_nM_\alpha E_nE_\alpha)^{\frac{1}{2}}(\cos\theta)/M_R, \quad (4)$$

where Q_0 is the energy released in going to the ground level. The excitation energy is thus dependent on two measured quantities only, the angle θ and the alpha track length.

The number of forks in which a given excitation energy was found was plotted *versus* the excitation energy. Two conditions were applied to all disintegration forks used: (1) the range of the heavy particle in a disintegration was required to lie within 0.1 cm of the mean value of the range for that energy; (2) the computed angle of recoil of the heavy particle and the measured angle were required to agree within 10°.

TABLE I. Excitation energies for C^{13} from the $O^{16}(n,\alpha)C^{13}$ reaction and from the $C^{12}(d,p)C^{13}$ reaction.

Levels found here Mev	Levels found by Rotblat Mev
3.0	3.1
3.7	3.7
	3.9
	6.3
	6.9
	7.6
	7.9
	8.3

$O^{16}(n,\alpha)C^{13}$

From the mass value tables of Li, Whaling, Fowler, and Lauritsen[9] one finds the Q_0 for this reaction to be -2.2 Mev. With 14.1-Mev neutrons the maximum possible excitation of the residual C^{13} nucleus is 11.0 Mev. Owing to the low penetrability[10] of the alpha-particles when the C^{13} is left highly excited (0.3 at 8.2 Mev and 4×10^{-5} at 10.3 Mev excitation of the C^{13}), the cross section is reduced so that the reaction may not be observed in this region. Figure 5 gives the number of disintegration forks as a function of excitation energy of the residual C^{13} nucleus. Positions of levels as reported by Rotblat[11] are indicated by dotted lines.

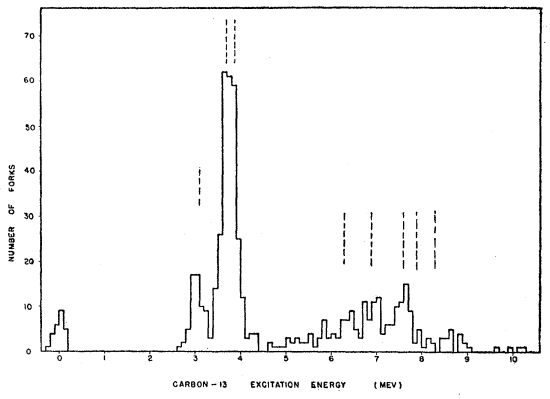

FIG. 5. The number of disintegrations in the $O^{16}(n,\alpha)C^{13}$ reaction as a function of the excitation energy of the residual C^{13} nucleus. The dotted lines indicate the positions of levels reported by Rotblat.

The first two levels at 3.0 Mev and 3.7 Mev agree with those of Rotblat at 3.1 Mev and 3.7 Mev, although there is no indication of a doublet at 3.7 Mev. Malm and Buechner,[12] studying the $N^{15}(d,\alpha)C^{13}$ reaction, have placed these levels at 3.083 and 3.677 Mev, respectively. No group is found corresponding to a level at 1 Mev as reported by others.[13,14] The higher levels have not been resolved.

Table I gives the levels found here and those reported by Rotblat.

Figures 6 and 7 show the angular distributions of the alpha-particles from the 3.0 Mev and 3.7 Mev levels, respectively. Each distribution has been fitted with a Legendre polynomial series, and this latter curve is shown by the smooth line. From the large orders of polynomials required for these fits (10 for the 3.0-Mev group and 8 for the 3.7-Mev group) one concludes that angular momenta of orders 5 and 4, respectively, are

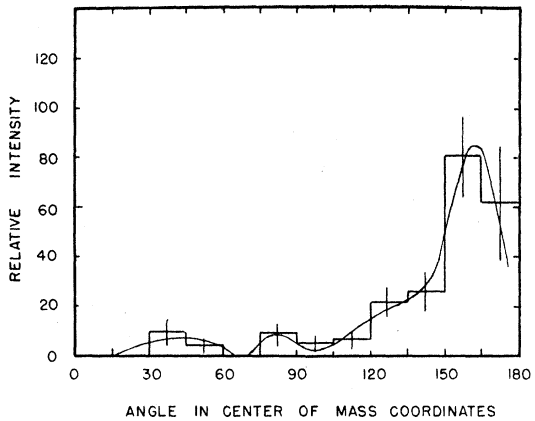

FIG. 6. The angular distribution in the center-of-mass system of alpha-particles emitted in the $O^{16}(n,\alpha)C^{13}$ reaction, which leave the C^{13} nucleus excited to 3.0 Mev. The solid curve is a Legendre polynomial series expansion of order 10 fitted to the histogram.

[8] P. M. S. Blackett, Proc. Roy. Soc. (London) **A134**, 669 (1932).
[9] Li, Whaling, Fowler, and Lauritsen, Phys. Rev. **83**, 512 (1951).
[10] Bloch, Hull, Broyles, Bouricius, Freeman, and Breit, Revs. Modern Phys. **23**, 147 (1951).
[11] J. Rotblat, Harwell Conference (1950).
[12] R. Malm and W. W. Buechner, Phys. Rev. **81**, 519 (1951).
[13] I. B. Berlman, Phys. Rev. **79**, 411 (1950).
[14] K. Boyer, Phys. Rev. **78**, 345 (1950).

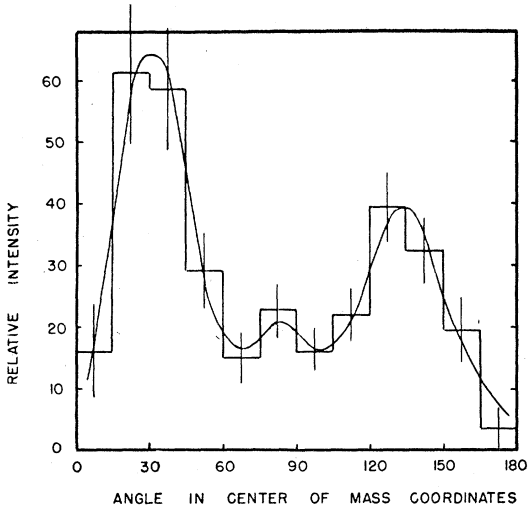

FIG. 7. The angular distribution in the center-of-mass system of alpha-particles emitted in the $O^{16}(n,\alpha)C^{13}$ reaction, which leave the C^{13} nucleus excited to 3.7 Mev. The solid curve is a Legendre polynomial series expansion of order 8 fitted to the histogram.

probably involved and that the compound states of O^{17} involved are states of high angular momentum.

The group at 3.7 Mev was divided into two parts, those with C^{13} excitations above 3.7 Mev and those with C^{13} excitations below. The angular distributions for these two groups were essentially the same, indicating that all the forks were probably due to one level and not to a doublet. The angular distribution for this level is similar in shape to those predicted by Butler's stripping theory, although there is apparently no reason for this.

$N^{14}(n,\alpha)B^{11}$

From the mass value tables, the Q_0 for the reaction $N^{14}(n,\alpha)B^{11}$ is found to be -0.2 Mev. The maximum excitation energy of the B^{11} nucleus possible with the 14.1-Mev neutrons is 12.9 Mev. Again, owing to the low penetrability of the alphas when the B^{11} is left highly excited, the reaction cross section may be expected to become small. Figure 8 shows the number of forks as a function of the excitation of the B^{11}. Known levels, as reported by Van Patter *et al.*[15] from a study of the reaction $B^{10}(d,p)B^{11}$, are indicated by arrows.

The level at 8.0 Mev, which was not found by Van Patter, may correspond to a level found at 7.82 Mev by Bateson[16] using the $B^{10}(d,p)B^{11}$ reaction and by Fulbright and Bush[17] who studied the inelastic scattering of protons.

In the region of excitation of the B^{11} from 8.3 Mev to 11.7 Mev, the penetrability of the alpha-particles drops a factor of 25 from 0.67 to 0.026, and few tracks are found above $9\frac{1}{2}$ Mev. At 11.8 Mev, however, a large group does appear, which is much more intense than the lower levels found.

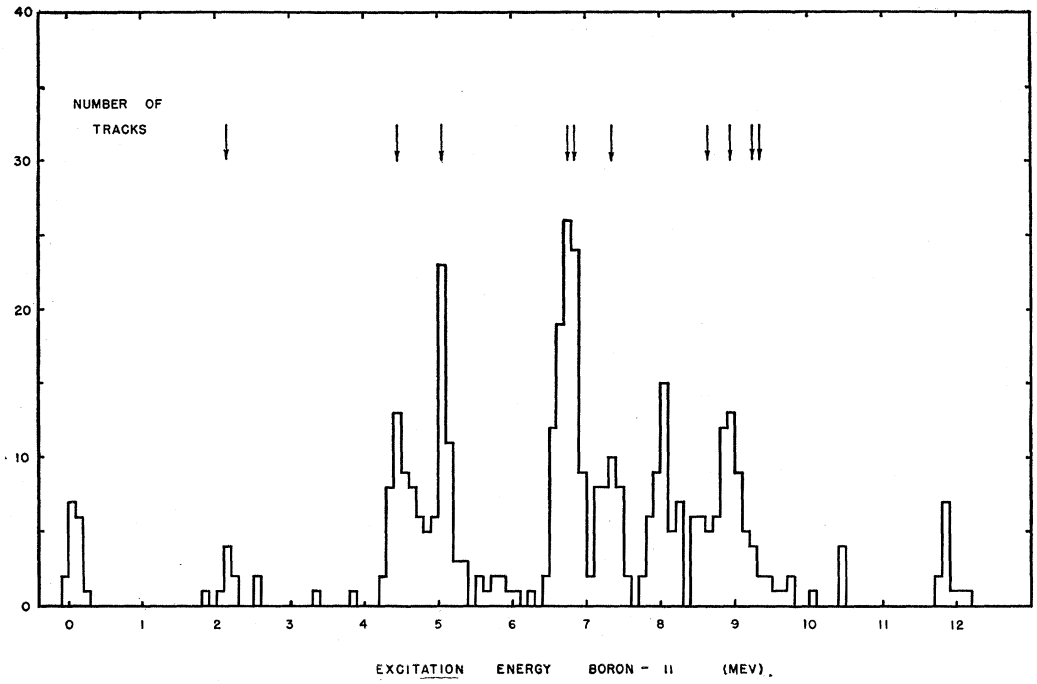

FIG. 8. The number of disintegrations in the $N^{14}(n,\alpha)B^{11}$ reaction as a function of the excitation energy of the residual B^{11} nucleus. The arrows indicate the positions of levels reported by Van Patter *et al.*

[15] Van Patter, Buechner, and Sperduto, Phys. Rev. **82**, 254 (1951).
[16] W. O. Bateson, Phys. Rev. **80**, 984 (1950).
[17] H. W. Fulbright and R. R. Bush, Phys. Rev. **74**, 1323 (1948).

Table II gives the levels as found here and those reported by Van Patter.

While a sufficient number of tracks to permit a detailed study of the angular distributions and hence the angular momenta involved was unavailable in these alpha-groups, it was felt that the distributions were worth tabulating. Table III gives these distributions, corrected for solid angle, for each group of alphas found in Fig. 8, listed according to the range of excitation energies in each group. Most of the distributions are not spherically symmetric, but there does not appear to be any particularly preferred direction for the maximum intensity.

$O^{16}(n,p)N^{16}$ and $O^{16}(n,d)N^{15}$

The Q_0 for the reaction $O^{16}(n,d)N^{15}$ is -9.9 Mev. The Q_0 for the $O^{16}(n,p)N^{16}$ reaction is not accurately known. A value of this Q may be determined, however, by using the Q value -0.034 Mev for the $N^{15}(d,p)N^{16}$ reaction determined by Malm and Buechner,[18] assuming that this Q relates to the ground level transition and not to an excited state of N^{16}. This gives the Q_0 for the $O^{16}(n,p)N^{16}$ reaction equal to -9.9 Mev. Maximum excitations of the residual N^{15} and N^{16} nuclei of 3.3 Mev are possible in each case.

TABLE II. Excitation energies for B^{11} found here from $N^{14}(n,\alpha)B^{11}$ reaction, and those found by Van Patter studying the $B^{10}(d,p)B^{11}$ reaction using magnetic analysis.

Levels found here Mev	Levels found by Van Patter Mev
2.1	2.138
4.4	4.459
5.0	5.034
6.7	6.758
	6.808
7.3	7.298
8.0	
8.5	8.568
8.9	8.926
	9.190
	9.276
11.8	

It is difficult to distinguish proton reactions from deuteron reactions, since the density of a proton track and the density of a deuteron track of the same range are approximately the same, and the other criteria used above were not decisive. The reactions were accordingly computed first as all being proton reactions and then as all being deuteron reactions. Four groups were found of which three could be assigned to known levels in one or the other of the two nuclei. Figure 9 shows three of these groups assigned to N^{16}. The fourth group was due to the ground level transition in the reaction $O^{16}(n,d)N^{15}$. Dotted lines indicate the positions of known levels. The group at 1.7 Mev probably corresponds to the level at 1.6 Mev reported by Bleuler and Rossel.[19] The general spread near the ground level could be due to the level at 0.3 Mev reported by Wyly.[20]

[18] R. Malm and W. W. Buechner, Phys. Rev. **80**, 771 (1950).
[19] E. Bleuler and J. Rossel, Helv. Phys. Acta **20**, 445 (1947).

TABLE III. The number of alpha-particles emitted at different laboratory angles for the $N^{14}(n,\alpha)B^{11}$ reaction. These are tabulated according to groups as found in Fig. 8.

Group with B^{11} excitation energy	Angle of emission of α-particles (laboratory system) 0–30	30–60	60–90	90–120	120–150	150–180
−0.1 to 0.2	0	0	1	6	13	9
4.3 to 4.6	0	14	13	7	8	14
4.7 to 5.1	20	10	8	8	15	10
6.5 to 6.9	10	17	27	25	34	14
7.1 to 7.4	3	8	10	16	4	0
7.8 to 8.2	15	5	6	13	23	16
8.4 to 9.4	15	29	22	16	7	5
10.4	0	1	1	1	2	0
11.7 to 12.1	10	3	3	0	5	0

Assigning the groups to certain reactions is not purely arbitrary. One factor considered is whether a group agrees with the position of a known level in one nucleus but does not agree with any level in the other nucleus. This was the case with three of the four groups found. Two agree with known levels in N^{16} (ground level and 1.6-Mev level), and one agrees with the ground level of the N^{15}. In general, if a group due to one reaction is misinterpreted as being due to the other reaction, the group on the excitation energy histogram will be smeared out. Thus, the group shown at 2.6 Mev for N^{16} and which has a spread of 0.7 Mev had a spread of 2 Mev when computed as being due to the n–d reaction. Also, this group did not correspond to a known level in either nucleus—there being no known levels in N^{15} up to 5.3 Mev. This might, of course, be a high-spin state of excited N^{15} which had not been found by reactions involving slower charged particles. Finally, the group near the ground level of N^{16}, when computed as due to the n–d reaction, led to negative excitation energies which are impossible.

Table IV lists the levels found here together with those reported elsewhere.

$N^{14}(n,p)C^{14}$, $N^{14}(n,d)C^{13}$, $N^{14}(n,t)C^{12}$

The disintegration of N^{14} gives rise to three reactions with the emission of hydrogen nuclei: $N^{14}(n,p)C^{14}+0.6$

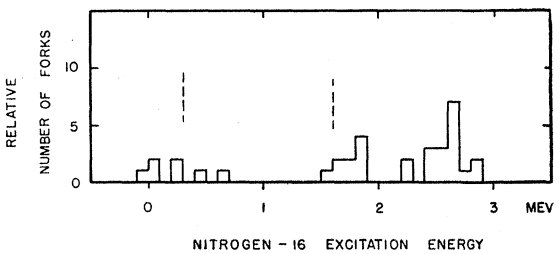

FIG. 9. The number of disintegrations in the $O^{16}(n,p)N^{16}$ reaction as a function of the excitation energy of the residual N^{16} nucleus. The dotted lines indicate the positions of levels reported by Wyly at 0.3 Mev and by Bleuler and Rossel at 1.6 Mev.

[20] L. D. Wyly, Phys. Rev. **76**, 316 (1949).

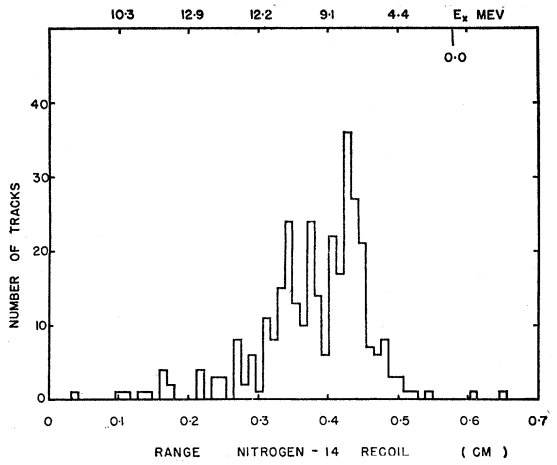

FIG. 10. The number of recoil N^{14} nuclei struck by 14.1-Mev neutrons as a function of the range of the recoil nuclei. All recoil nuclei measured lay within a cone of 15° half-angle with respect to the neutron's path. The scale at the top is the calculated excitation energy of the recoil.

Mev, $N^{14}(n,d)C^{13}-5.3$ Mev, and $N^{14}(n,t)C^{12}-4.0$ Mev. The last of these reactions will not likely be measured, however, since tritons leaving the C^{12} in the 4.5-Mev or ground levels are too energetic and will not be stopped in the chamber. On the other hand, a group from the next higher known level at 9.7 Mev is not energetically possible. Only if there were an intermediate level would the tritons actually stop in the chamber. The protons and deuterons emitted have long ranges and also will not be stopped in the chamber in some cases. However, the protons can stop in the chamber when the C^{14} is left excited above $9\frac{1}{2}$ Mev (13.8-Mev excitation is possible), and the deuterons can stop in the chamber if the C^{13} is left excited above $1\frac{1}{2}$ Mev (7.9-Mev excitation is possible).

Since the proton, deuteron, and triton reactions cannot be distinguished from each other by the appearance of the tracks, all these hydrogen reactions were computed first as n–p and then as n–d reactions. Groups could be seen in each case but were not entirely resolved. As a result, the positive identification of the reactions was not possible here as in the n–p and n–d reactions in O^{16}.

3. Recoils

When a neutron strikes an oxygen or nitrogen nucleus it may be scattered elastically or inelastically, and the event observed as a short heavy recoil in the cloud chamber. By measuring the length of the recoil track (and thus getting its energy) and the recoil angle from the neutron's path, the excitation energy of the recoiling particle can be determined. Figure 10 shows the number of nitrogen recoils in the forward direction *versus* the range of the recoil. The top scale is the corresponding excitation energy. In a collision process

$$E_x=-(M_n+M_R)E_R/M_n+2(M_RE_nE_R/M_n)^{\frac{1}{2}}, \quad (5)$$

where the recoil is at zero degrees to the neutron's path, and E_x is the excitation energy of the recoil particle. The energy E_R of the recoil can be derived from the track length by using Eq. (3) and by comparing with the range-energy curve of C^{13} of Fig. 3.

For elastic scattering of the neutron through 180°,

$$E_R=4M_RM_n(M_R+M_n)^{-2}E_n. \quad (6)$$

With 14.1-Mev neutrons, this gives $E_R=3.5$ Mev. The range of the recoil with this energy, using Eq. (3) with $n=0.5$, is $R=0.58$ cm.

The track lengths to be measured are very short, and the relative errors are large. It can be seen, however, that the number of elastically scattered neutrons is very small with respect to the number of inelastically scattered neutrons for recoils lying less than 15° from the neutron's path.

Similar results were found for oxygen recoils although the number of tracks involved was smaller.

TABLE IV. Excitation energies for N^{16} found here from the $O^{16}(n,p)N^{16}$ reaction, and levels reported elsewhere.

Levels found here Mev	Levels reported elsewhere Mev
0.3?	0.3[a]
1.7	1.6[b]
2.6	

[a] See reference 20.
[b] See reference 19.

4. Cross Sections

To compute the value of the cross section for a reaction, the number of times the reaction occurs is compared to the number of recoil protons occurring in the same number of pictures. Since the relative number of oxygen (or nitrogen) and hydrogen nuclei present are known and since the neutron flux is the same for all reactions, the ratio of the cross section for this reaction to that for n–p scattering can be determined. A value of 0.675 barns[21] for the n–p scattering was used.

In the disintegration of oxygen the cross section for alpha-emission is 310 millibarns. The cross sections for proton emission and deuteron emission are 35 and 15 millibarns.

In the disintegration of nitrogen the cross section for alpha-emission is 100 millibarns. Since it is difficult to distinguish between proton, deuteron, and triton tracks, these reactions have been grouped together with a total cross section of 100 millibarns. The cross section for the disintegration of the nitrogen into Li^7 and two alpha-particles is 15 millibarns.

[21] R. K. Adair, Revs. Modern Phys. **22**, 249 (1950).

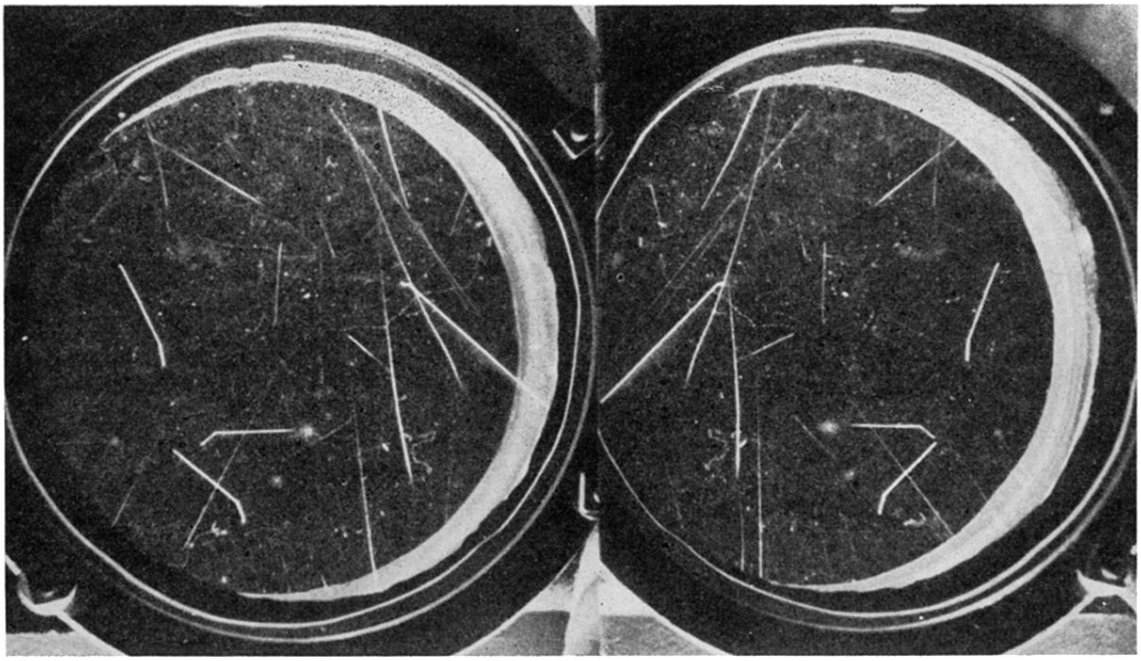

FIG. 1. Stereoscopic picture of disintegrations in oxygen. The neutrons enter from the top of the picture. Several examples of disintegration with alpha-emission can be noted.

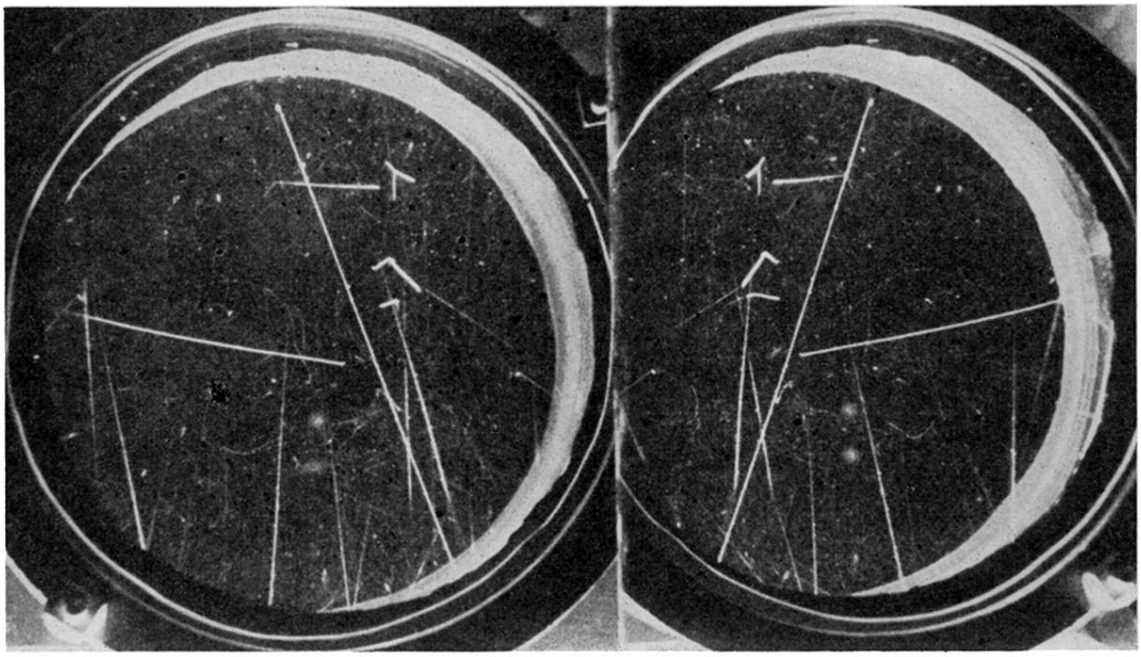

FIG. 2. Stereoscopic picture of disintegrations in nitrogen. The neutrons enter from the top of the picture. Two cases of three-particle disintegration can be seen, as well as a disintegration in which either a proton or deuteron or triton is emitted which crosses and leaves the chamber. Some recoil nitrogen nuclei identifiable as short heavy tracks and an example of alpha-emission are also seen.